



# Electron-vibrational relaxation of photoexcited polyfluorenes in the presence of chemical defects: A theoretical study

Ignacio Franco<sup>a,b</sup>, Sergei Tretiak<sup>a,\*</sup>

<sup>a</sup> *Theoretical Division and Center for Nonlinear Studies, Los Alamos National Laboratory, Mail stop B268, Los Alamos, NM 87545, USA*

<sup>b</sup> *Abdus Salam International Centre for Theoretical Physics, Trieste 34014, Italy*

Received 26 February 2003

## Abstract

A quantum chemical semiempirical investigation of electron-vibrational dynamics of photoexcited conjugated polyfluorenes shows that delocalized electronic excitations dominate the absorption, whereas chemical defects (if present) dramatically impact the emission by trapping the photogenerated exciton into a localized state and acting as guest emitters at recombination. These results offer theoretical insight into the effect of non-quenching defect sites in conjugated polymers and explain the origin of a controversial low energy emission band frequently observed in bulk polyfluorene samples.

© 2003 Elsevier Science B.V. All rights reserved.

Light emitting conjugated polymers are of interest both for their broad technological applications [1–4] and because they are model systems to gain fundamental understanding of the properties of soft organic and biological matter. Almost every photochemical, photophysical or spectroscopic process in these materials involve dynamics of photoexcited states and, for this reason, its theoretical characterization has immediate technological implications and offers valuable insight into the nature and behavior of excitations in soft materials.

Polyfluorenes (PF) and their derivatives have received a great deal of attention lately and are evolving as a major class of materials for light emitting diodes (LEDs) [5–7]. They exhibit a very attractive pure blue emission [5], an efficient electroluminescence [8,9], a high carrier mobility [10] and a good processability [6]. The building blocks of PF are rigid planar biphenyl units, bridged by a non-conjugated carbon atom (Fig. 1a). Its typical absorption spectrum has a strong featureless peak at about 3.25 eV [5,6] corresponding to the  $1B_u$  (band-gap) state absorption. The blue emission of the polymer in solution shows a well resolved vibrational structure with the 0–0 transition at 2.98 eV being the most intense [5,6].

\* Corresponding author. Fax: +1-505-665-3909.  
E-mail address: [serg@cns.lanl.gov](mailto:serg@cns.lanl.gov) (S. Tretiak).

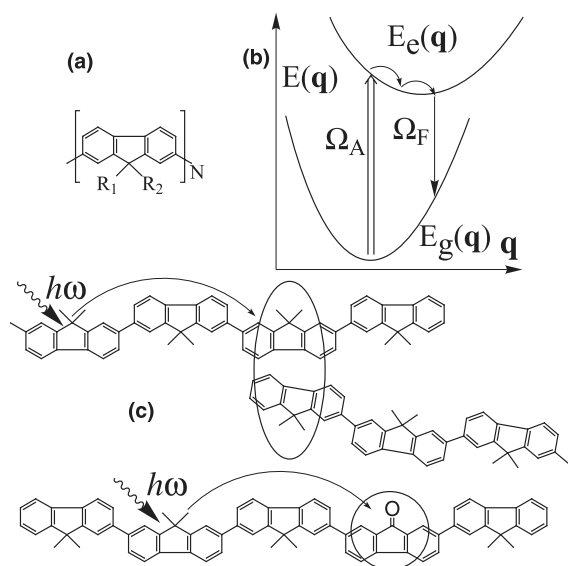


Fig. 1. (a) Structure of polyfluorene. (b) Schematic representation of photoexcitation dynamics.  $\Omega_A$  and  $\Omega_F$  are vertical absorption and fluorescence transition energies, respectively;  $E_g(\mathbf{q})$  and  $E_e(\mathbf{q})$  represent the energy as a function of nuclear coordinates  $\mathbf{q}$  for the ground and excited states, respectively. (c) Excimer formation due to aggregation (upper scheme) and chemical keto defects (lower scheme) are proposed hypotheses for the origin of the yellow emission in PF.

It is generally believed that the role of chemical (keto) defects in conjugated polymers is to quench the emission properties by trapping the photoinduced excitons turning them into non-emissive species [11]. In this Letter, we report a quantum chemical investigation of the dynamics of photoexcited conjugated polyfluorenes with and without keto defects. In contrast to the mechanism proposed by Yan et al. [11], our results suggest that oxidative defects do not quench the emission; they trap the photoinduced exciton and act as guest emitters at the moment of recombination introducing in this way a novel strong low energy band in the fluorescence spectra of the polymer. A similar parasite band has been observed in bulk PF samples in the yellow region of the spectrum (2.2–2.3 eV) [12] turning the desired blue emission into a green color. Its origin has been the subject of recent controversy. Traditionally it has been assigned to aggregation and/or excimer formation in the solid state samples [13–15] (see Fig. 1c). This

interpretation has had a tremendous impact in the literature (e.g., the work of Lemmer et al. [13] has been cited over 100 times). However, a second hypothesis, clearly supported by the results reported herein, has been recently proposed by List and Scherf [6,12] and Lupton and collaborators [16]. They have presented experimental evidence that suggests that chemical fluorenone (keto) defects, and not aggregates, are responsible for the novel yellow band emission (Fig. 1c). They have also shown that these defects can readily be formed during synthesis of the polymer and operation of the devices [6,12]. Previous quantum chemical studies have focused on the excited state electronic structure of pristine PF and similar polymers [17,18] and the role of chemical defects in PF has been addressed in a recent experimental–theoretical study [19].

We investigated the electronic structure and spectroscopic properties of two PF oligomers (shown in Fig. 2a). The first one consists of five fluorene units and was used to study pristine PF properties. Hereafter we will refer to this structure as O1. Keto-doped PF were simulated with an oligomer seven units long, where the second to the last monomer contains a defect site. We will refer to this molecule as O2.

We focus on the lowest singlet excited  $1B_u$  (band-gap) state as it is the most important one in uv–vis spectra. As schematically shown in Fig. 1b, when a molecule (initially being in the relaxed ground state geometry) absorbs a photon (vertical absorption  $\Omega_A$ ) an electron–hole pair (exciton) is created. This initial photoexcitation (hot exciton) subsequently relaxes along the excited state potential energy hypersurface of the oligomer  $E_e(\mathbf{q})$  distorting the molecular geometry in the process. During emission the resulting ‘cold exciton’ recombines and the system decays radiatively back to the ground state from the excited state optimal geometry (vertical fluorescence  $\Omega_F$ ).

To study the absorption and emission properties of O1 and O2 we employed the following computational strategy: Ground state optimal geometries were obtained with the Austin Model 1 (AM1) semiempirical Hamiltonian [20], which is specifically designed for this purpose. To find the excited state equilibrium geometries we used a

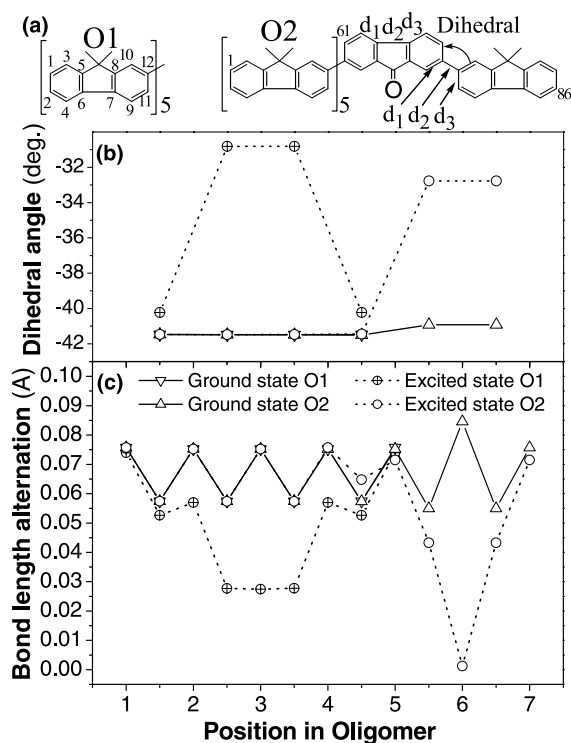


Fig. 2. (a) Structures of undoped (O1) and keto-doped (O2) PF oligomers. Variation of (b) the dihedral angle and (c) bond length alternation parameter (defined as  $(d_2 - (d_1 + d_3))/2$ ) along the oligomer chain for the ground and excited state relaxed geometries in O1 and O2.  $X$ -axis labels consecutive monomers (half-integers correspond to positions between monomers) as shown in (a).

recently developed excited state molecular dynamics approach [21], which calculates trajectories on the excited state molecular potential energy hypersurface. In this method the excited state potential energy gradients are obtained quantum mechanically rather than classically using the Collective Electronic Oscillators (CEO) technique [22]. The CEO combines semiempirical Hamiltonians with a time-dependent Hartree Fock formalism, and utilizes numerically efficient Krylov space algorithms making the computation of excited states not substantially more numerically demanding than the ground state. In particular, the computational efficiency of the CEO combined with AM1 Hamiltonian allowed us to find the lowest excited state optimal geometries in such large molecular systems as O1 and O2. The ground

and excited state optimal structures allows to calculate vertical transition energies and subsequently to obtain vibrationally resolved absorption and fluorescence lineshapes [21]. We used the Intermediate Neglect of Differential Overlap/Spectroscopy Hamiltonian [23] (which has been specifically parameterized for computing *uv-vis* spectra of organic molecules) and the CEO for calculating the spectroscopic observables relevant to the absorption and emission spectra of O1 and O2 (note that AM1/CEO approach reproduce all trends described below with a consistent shift of all transition energies to the red by  $\sim 0.3$  eV).

We first examine structural changes induced by photoexcitation in both oligomers, which typically can be characterized by dihedral angle and bond length alternation parameters [18,21] (Fig. 2a). The ground state for O1 is not planar (Fig. 2b). Interactions between fluorene units result in a twisted configuration with a  $\sim 41^\circ$  dihedral angle between monomers, which agrees well with the experimental value of  $\sim 36^\circ$  [6]. When going to the excited  $1B_u$  state, O1 acquires a more planar conformation in the middle of the molecule improving  $\pi$  conjugation between the three inner fluorene units. The bond length alternation parameter measures the uneven distribution of  $\pi$  electrons over the bonds (Peierls distortion). Fig. 2c shows that bond length alternation in O1's ground state geometry is constant for equivalent bonds along the chain, and noticeably reduced in the middle of the molecule for the  $1B_u$  excited state geometry. As previously observed in poly(*p*-phenylene vinylene) [21], this localized reduction of dihedral angles and bond length alternation is a characteristic signature of an exciton self-trapping. The confinement of the excitation in the 3 middle fluorenes in O1 by vibrational relaxation is clearly reflected on the size-scaling behavior of vertical absorption and fluorescence energies. As shown in the left panel of Fig. 3, both  $\Omega_A$  and  $\Omega_F$  saturate to a constant value with increasing the chain length and O1 mimics well the long-chain limit. Fluorescence, however, saturates faster than absorption because the relaxed exciton compromises only part of the oligomer while the hot exciton is delocalized along the whole chain. This feature is evidenced in oscillators strengths (right panel) as a

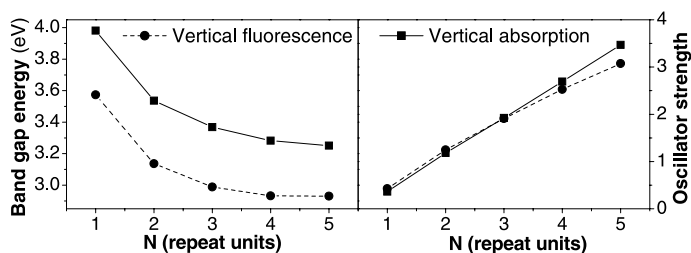


Fig. 3. Variation of vertical absorption and fluorescence transition frequencies (left panel) and their corresponding oscillator strengths (right panel) with the number of repeat units in pristine PF oligomers.

deviation from linear scaling with the system size for the fluorescence as compared to the absorption.

The introduction of a keto defect into the system (O2) does not affect significantly the ground state geometry (Fig. 2b and c). Drastic changes arise, however, when going to the excited state: A planarization of the molecule is observed in the neighborhood of the defect site and a reduction of the bond length alternation is clearly seen in this unit itself. Practically all bond lengths become even on the fluorenone promoting maximum electronic delocalization on the defect unit. Moreover, the first five fluorene units in O2 remain virtually unaltered compared to the ground state geometry. The fact that geometry changes are only observed in the neighborhood of the defect site upon excitation, and not along the pristine conjugated portion of the molecule, indicates a trapping of the exciton by the defect.

To connect these structural changes with distinct dynamics of the underlying photoinduced electron–hole pairs in doped and undoped oligomers we further use two-dimensional real-space analysis of the transition densities [22,24] related to the absorption and emission electronic spectra of O1 and O2 (Fig. 4). These quantities are given as  $(\xi_v)_{mn} = \langle v | c_m^+ c_n | g \rangle$  where  $c_m^+$  ( $c_m$ ) are creation (annihilation) operators of an electron at the  $m$ th atomic orbital, and  $|g\rangle$  ( $|v\rangle$ ) is the ground (excited) state many-electron wavefunction [22,24]. The diagonal elements  $(\xi_v)_{nn}$  represent the net charge induced in the  $n$ th atomic orbital by the external field. The off-diagonal elements  $(\xi_v)_{mn}$  with  $m \neq n$  represent the joint probability amplitude of finding an electron and a hole located at the  $m$ th and  $n$ th

atomic orbitals, respectively. Thus, the transition densities provide a real-space picture of electronic transitions by showing accompanying motions of optically induced charges and electronic coherences [22,24].

The exciton created by  $1B_u$  state absorption in O1 (Fig. 4a) is delocalized over the entire chain (diagonal in the plot). The exciton size (maximal distance between the electron and the hole) is about 1.5–2 repeat units (largest off-diagonal extent of the non-zero matrix area). The exciton diagonal size decreases from 5 to  $\sim 3$ –3.5 repeat units at the excited state geometry (Fig. 4a'). This confirms exciton self-trapping by vibrational relaxation in the middle of the chain. However, the exciton is still sufficiently delocalized so that a considerable portion of the oligomer participates in the emission. In addition, after relaxation the exciton size increases to  $\sim 2$ –2.5 repeat units due to the enhanced local conjugation promoted by planarization of the middle portion of the chain (compare Fig. 2a and b). Vibrational relaxation leads to 0.3 eV Stokes shift in O1, however, the oscillator strength does not change significantly (Table 1). Overall calculated absorption and emission transition energies show an excellent agreement with experiment (Table 1).

In contrast to O1, the lowest excited state (O2(I)) created by an absorbed photon in O2 does not correspond to the band-gap  $1B_u$  state. The exciton has the center of mass at the defect site (Fig. 4b) and is delocalized over the defect and its two neighboring units. The O2(I) state lies lower in energy and has a smaller oscillator strength than  $1B_u$  state in O1 (Table 1). We identify the third excited state (O2(II)) in O2 (Fig. 4c) as corre-

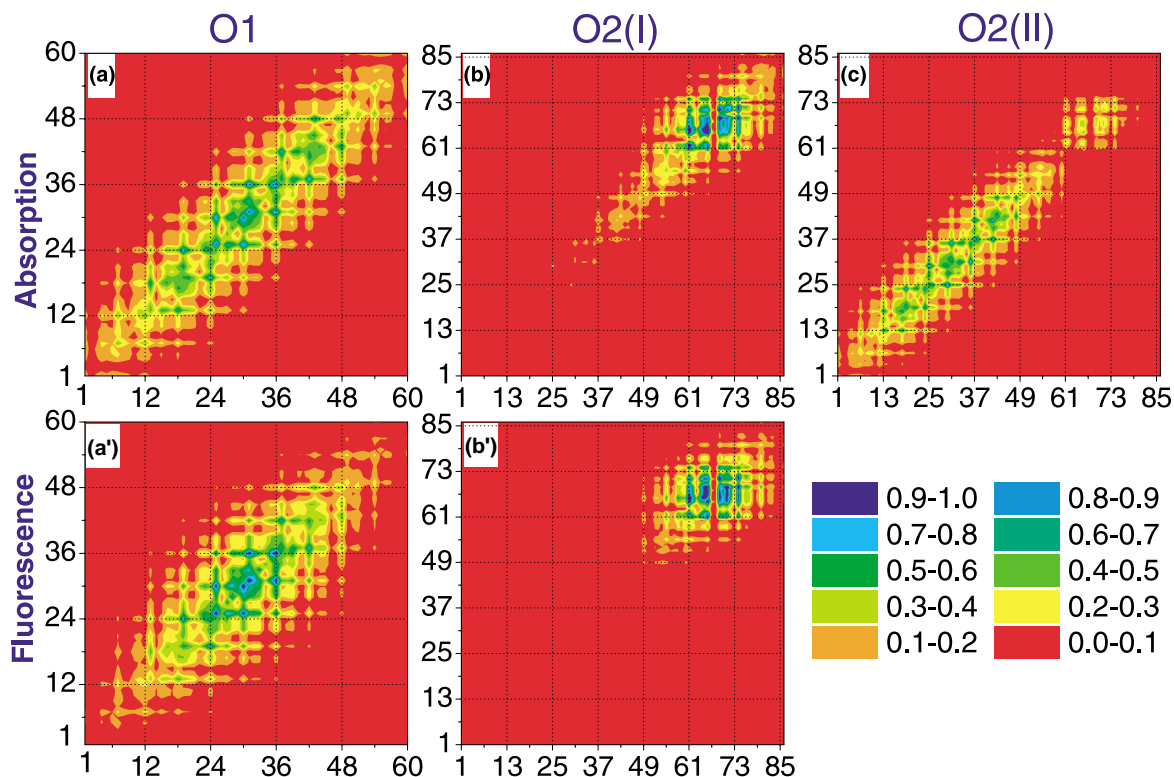


Fig. 4. Contour plots of transition density matrices of O1 and O2. (a)–(c) represent transitions from the ground state (equilibrium geometry) to the lowest excited state (third excited state for (c)) in O1 and O2 and correspond to vertical absorption. (a'), (b') represent the same quantities as (a) and (b) but computed at the excited state equilibrium geometries, and correspond to vertical fluorescence. The axis labels represent the individual atoms in the numbering sequence shown in Fig. 2a. The color code is given in the lower right corner. Each plot depicts probabilities of an electron moving from one molecular position (horizontal axis) to another (vertical axis) upon electronic excitation.

Table 1  
Computed vertical absorption  $\Omega_A$  and fluorescence  $\Omega_F$  transition energies for O1 and O2

	Calculations		Experiment	
	$\Omega_A$ (eV)	$\Omega_F$ (eV)	$\Omega_A$ (eV)	$\Omega_F$ (eV)
O1	3.25 (3.5)	2.94 (3.1)	3.2–3.3	2.98
O2(I)	3.06 (1.6)	2.55 (0.9)		2.2–2.3
O2(II)	3.25 (3.1)		3.2–3.3	

The corresponding oscillator strengths are given in parentheses. Experimental values correspond to the maximum of the absorption/emission profiles reported in [6].

sponding to the  $1B_u$  state in pristine PF oligomer because they have the same transition energy and oscillator strength. Similar to O1, O2(II) is delocalized over five conjugated repeat units with some

participation of the defect unit (compare Fig. 4a and c). Note that for delocalized excitations the defect tends to dissect the oligomer into separate conjugated segments (Fig. 4c). The O2(II) state has a strong oscillator strength and will subsequently dominate the absorption spectrum of doped PF making it similar to that of pristine PF.

After absorption to the  $1B_u$  state, the excitation is likely to be transferred to the lowest state O2(I) localized on the defect site (Kasha's rule [25]) and/or through long-range Förster energy transfer mechanism [26] in solid state samples. The effect of vibrational relaxation induces further localization of the excitation on the defect site (Fig. 4b'). Thus, the emission of PF with chemical defects originates from the exciton completely localized on

the fluorenone unit which acts as a guest site for exciton recombination. For this reason, the emission properties of the doped polymer are not sensitive to the position of the defect site in the chain and justifies the model (O2) adopted. As shown in Table 1, our computations predict that the presence of keto impurities lowers the emission frequency of O2 by  $\sim 0.4$  eV compared to O1, introducing an undesired band which changes the blue emission of pristine PF. We also note that the oscillator strength of O2(I) is reduced after relaxation which results in decreased photoluminescence. The Stoke's shift in keto-doped oligomer ( $\sim 0.7$  eV) is much larger than that of pristine PF ( $\sim 0.3$  eV), i.e., in order to host the relaxed photoexcitation the bonding pattern on the defect unit changes due to vibrational reorganization (see Fig. 2). Assuming that the yellow band experimental fluorescence originates from the keto defects (Table 1), our computational results for O2 emission are shifted from experiment to the blue by  $\sim 0.3$  eV. This may be attributed to polarization effects caused by interaction between the carbonyl dipole moment and the dielectric medium which enhances photoexcitation relaxation.

In conclusion, we have theoretically studied the effects of chemical defects on the dynamics of excitations in PF. Our analysis identifies exciton self-trapping in pristine oligomers and a non-quenching localization of the excitation in oxidative defects which results in a dominant low energy fluorescence band. Our computational results agree well with experimental data and strongly support the proposal of List et al. [6,12], Lupton et al. [16], and recent calculations by Zojer et al. [19] for the controversial origin of the yellow emission observed in bulk PF samples.

### Acknowledgements

This work was performed under the auspices of the US Department of Energy. The authors thank Dr. J.M. Lupton, Dr. A. Saxena, Dr. R.L. Martin, and Dr. A.R. Bishop for their critical comments.

### References

- [1] A.J. Heeger, *Rev. Mod. Phys.* 73 (2001) 681.
- [2] R.H. Friend, R.W. Gymer, A.B. Holmes, J.H. Burroughes, R.N. Marks, C. Taliani, D.D.C. Bradley, D.A. dos Santos, J.L. Brédas, M. Logdlund, W.R. Salaneck, *Nature* 397 (1999) 121.
- [3] M.A. Baldo, M.E. Thompson, S.R. Forrest, *Nature* 403 (2000) 750.
- [4] R.H. Friend, *Pure Appl., Chem.* 73 (2001) 425.
- [5] D. Neher, *Macromol. Rapid Commun.* 22 (2001) 1366.
- [6] U. Scherf, E.J.W. List, *Adv. Mater.* 14 (2002) 477.
- [7] D. Katsis, Y.H. Geng, J.J. Ou, S.W. Culligan, A. Trajkovska, S.H. Chen, L.J. Rothberg, *Chem. Mater.* 14 (2002) 1332.
- [8] Q.B. Pei, Y. Yang, *J. Am. Chem. Soc.* 118 (1996) 7416.
- [9] A.W. Grice, D.D.C. Bradley, M.T. Bernius, M. Inbasekaran, W.W. Wu, E.P. Woo, *Appl. Phys. Lett.* 73 (1998) 629.
- [10] M. Redecker, D.D.C. Bradley, M. Inbasekaran, E.P. Woo, *Appl. Phys. Lett.* 73 (1998) 1565.
- [11] M. Yan, L.J. Rothberg, F. Papadimitrakopoulos, M.E. Galvin, T.M. Miller, *Phys. Rev. Lett.* 73 (1994) 744.
- [12] E.J.W. List, R. Guentner, P. Scandiucci de Freitas, U. Scherf, *Adv. Mater.* 14 (2002) 374.
- [13] U. Lemmer, S. Heun, R.F. Mahrt, U. Scherf, M. Hopmeier, U. Siegner, E.O. Gobel, K. Mullen, H. Bassler, *Chem. Phys. Lett.* 240 (1995) 373.
- [14] E. Conwell, *Trends Pol. Sci.* 5 (1997) 218.
- [15] M. Grell, D.D.C. Bradley, G. Ungar, J. Hill, K.S. Whitehead, *Macromolecules* 32 (1999) 5810.
- [16] J.M. Lupton, M.R. Craig, E.W. Meijer, *Appl. Phys. Lett.* 80 (2002) 4489.
- [17] G. Greczynski, M. Fahlman, W.R. Salaneck, N. Johansson, D.A. dos Santos, A. Dkhissi, J.L. Brédas, *J. Chem. Phys.* 116 (2002) 1700.
- [18] S. Karabunarliev, E.R. Bittner, M. Baumgarten, *J. Chem. Phys.* 114 (2001) 5863.
- [19] E. Zojer, A. Pogantsch, E. Hennebicq, D. Beljonne, J.L. Bredas, P.S. de Freitas, U. Scherf, E.J.W. List, *J. Chem. Phys.* 117 (2002) 6794.
- [20] M.J.S. Dewar, E.G. Zoebisch, E.F. Healy, J.J.P. Stewart, *J. Am. Chem. Soc.* 107 (1985) 3902.
- [21] S. Tretiak, A. Saxena, R. Martin, A. Bishop, *Phys. Rev. Lett.* 8909 (2002) 7402.
- [22] S. Tretiak, S. Mukamel, *Chem. Rev.* 102 (2002) 3171.
- [23] J. Ridley, M.C. Zerner, *Theor. Chim. Acta* 32 (1973) 111.
- [24] S. Mukamel, S. Tretiak, T. Wagersreiter, V. Chernyak, *Science* 277 (1997) 781.
- [25] M. Kasha, H.R. Rawls, M.A. El-Bayoumi, *Pure Appl. Chem.* 11 (1965) 371.
- [26] T. Förster, *Naturwissenschaften* 33 (1946) 166.